Low-nu Relative Flux and Prism issues

C. Distefano
LNS-INFN

On behalf of the INFN DUNE and R. Petti

DUNE Multi-Purpose Detector Workshop

Low-nu method

For $\nu<\nu_0$ (where $\nu_0<<E_\nu$): cross section is approximately constant as a function of neutrino energy.

We can measure the shape of the neutrino flux as a function of $E_{\nu.}$

$$\Phi \propto \frac{U(D_\nu - B_\nu)}{C_\nu \times \Delta E_\nu}$$

Where

D_ν: reconstructed events

B_ν: background predicted by the simulation

U: unfolding operation (energy smearing and acceptance)

ΔE_ν: width of the neutrino energy bin

C_ν: correction factor for the small E_ν dependence of the low-ν cross section

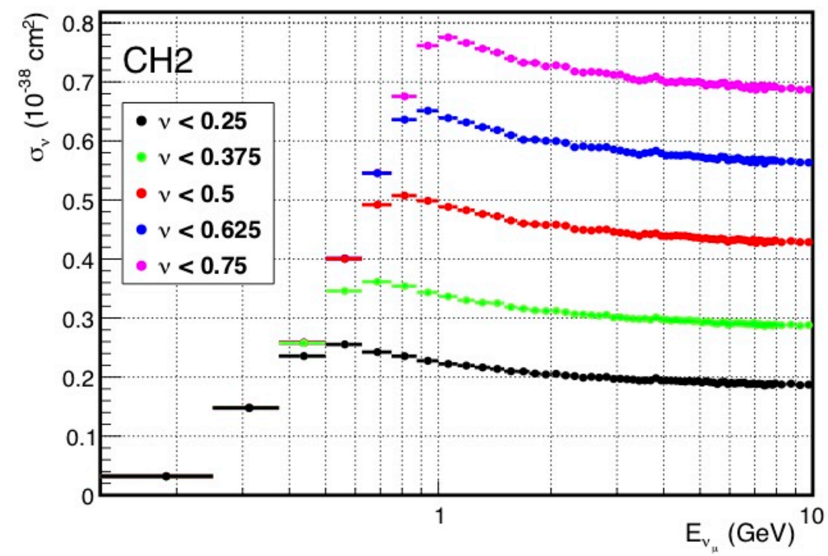

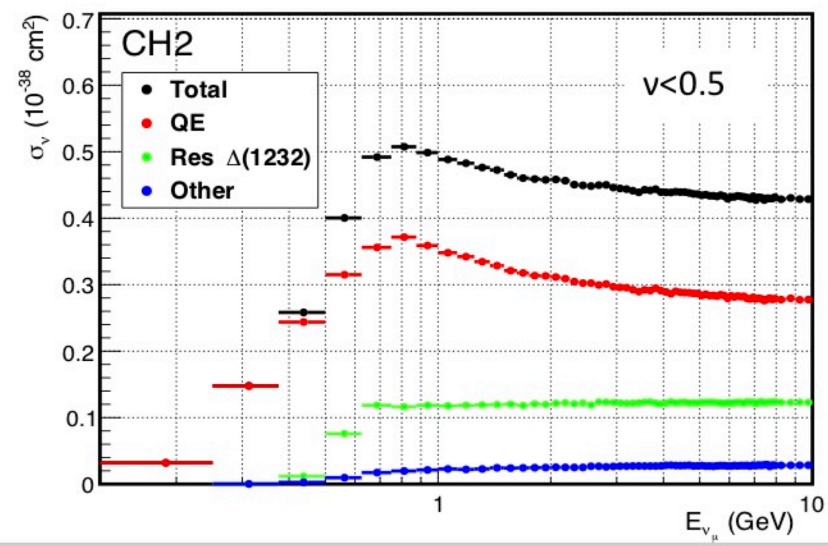

CH2 as target for low-nu analysis

Significant systematic uncertainties from nuclear effects and reconstruction of hadronic energy ν:

- total visible energy
- acceptance of the ν_0 cut used in the analysis

One example of such effects from neutron production, which are typically associated to some undetected energy

At small values of ν hadronic energy carried by neutrons is about a factor of 2 smaller in CH_2 than in Ar.

Similar results apply to the average number of neutrons produced.

Results confirmed by using different event generators, although large uncertainties are present on the neutron production

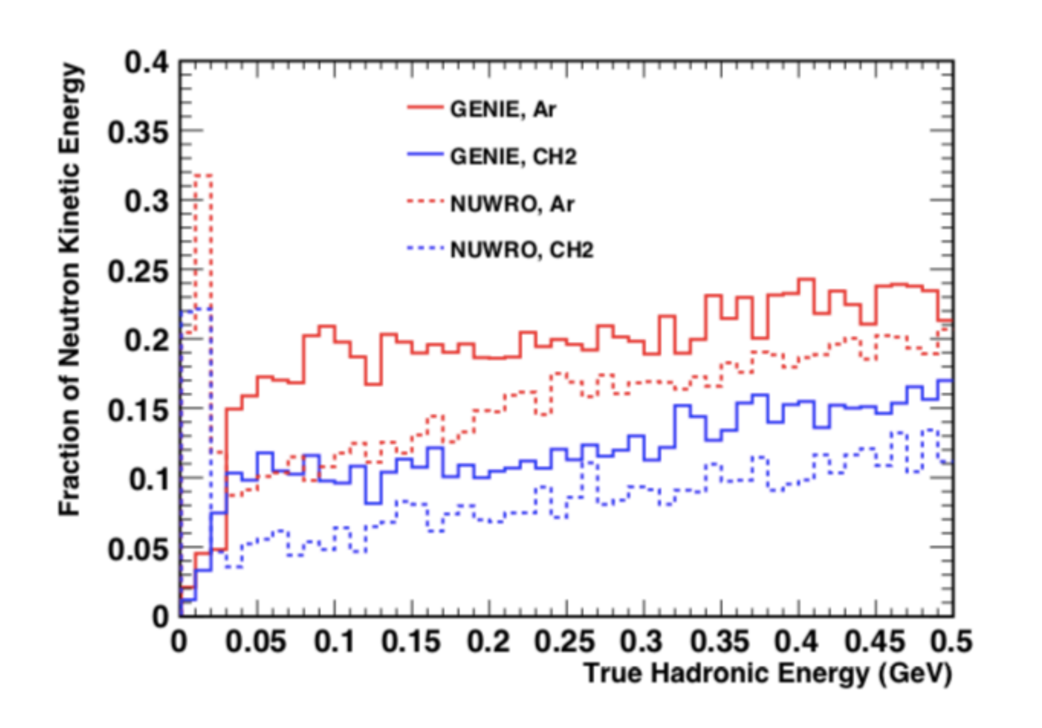

Interaction with hydrogen

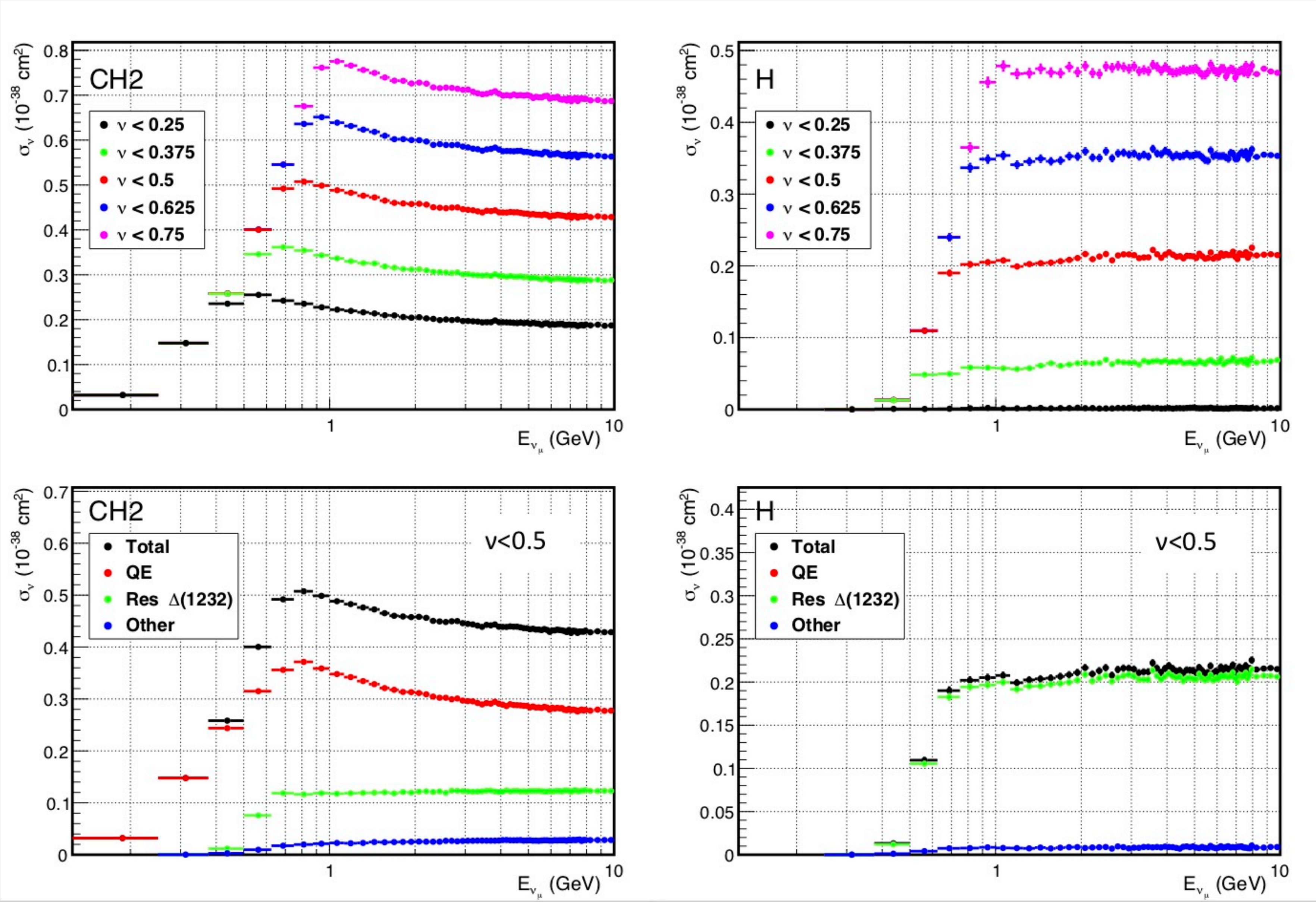

Choice of the ν_0 cut

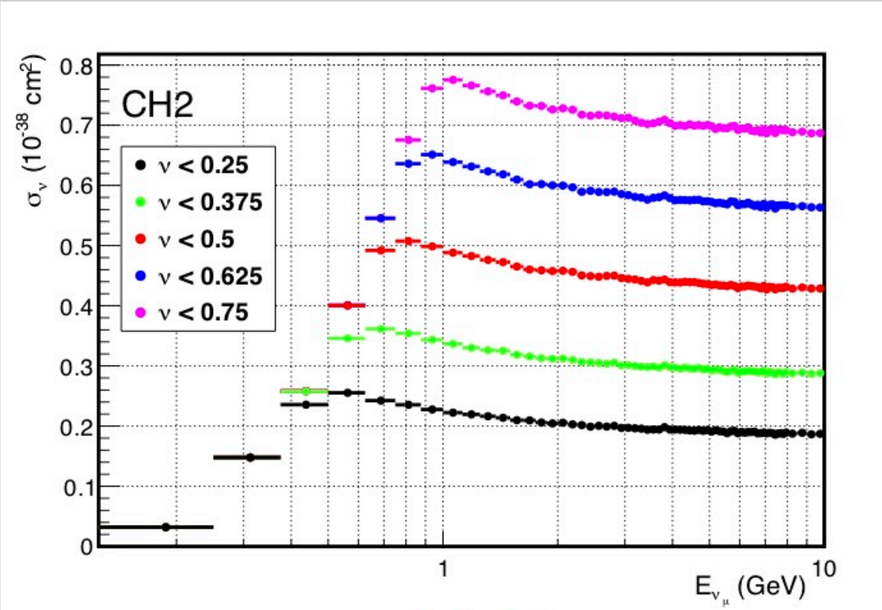

A larger ν_0 will select more data and yield smaller statistical uncertainties in the flux.

A smaller ν_0 will reduce the energy dependence of the low-ν cross section, and hence the flux-model dependence.

The minimum neutrino energy for each ν_0 cut is set to keep the low-nu events less than 50%

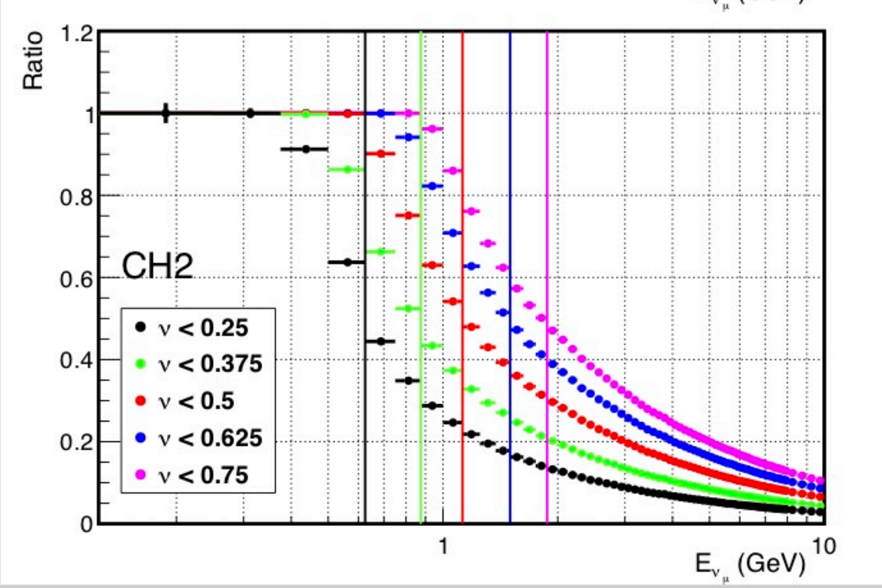

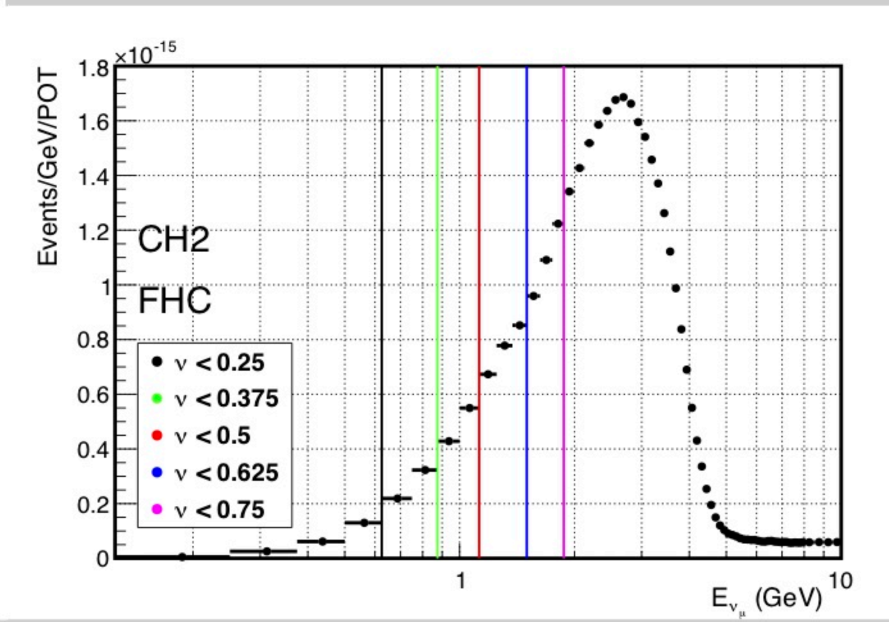

Simulations

Beam flux: 120 GeV proton, 1.1×10^{21} POT/year
Beam direction: theta=0.101 rad
Beam mode: FHC
Detector: KLOE inner tracker
Simulation based on GENIE 2.12.10

CH_2			
ν_0 (GeV)	E_{min} (GeV)	$N^{\nu}_{int}/5.5\cdot10^{21}$ POT	N^{ν}_{int}/N_{int}
0.250	0.625	$2.75\cdot10^{6}$	0.10
0.375	0.875	$3.97\cdot10^{6}$	0.14
0.500	1.125	$5.43\cdot10^{6}$	0.19
0.625	1.500	$6.23\cdot10^{6}$	0.22
0.750	1.875	$6.38\cdot10^{6}$	0.23
H			
ν_0 (GeV)	E_{min} (GeV)	$N^{\nu}_{int}/5.5\cdot10^{21}$ POT	N^{ν}_{int}/N_{int}
0.250	0.375	$2.83\cdot10^{3}$	0.00
0.375	0.500	$9.94\cdot10^{4}$	0.05
0.500	0.875	$3.10\cdot10^{5}$	0.14
0.625	1.250	$4.67\cdot10^{5}$	0.21
0.750	1.625	$5.45\cdot10^{5}$	0.25

Sample 1: used as *data*
Spectrum: beam
Exposure: 5 years (5.5×10^{21} POT)

Sample 2: used as *MC* truth
Spectrum: flat in energy

- Used to compute the correction factor

$$C_\nu = \frac{N(E_\nu, \nu < \nu_0)}{N(E_\nu \approx 10\ \text{GeV}, \nu < \nu_0)}$$

- Reweighed to the beam spectrum and used as MC

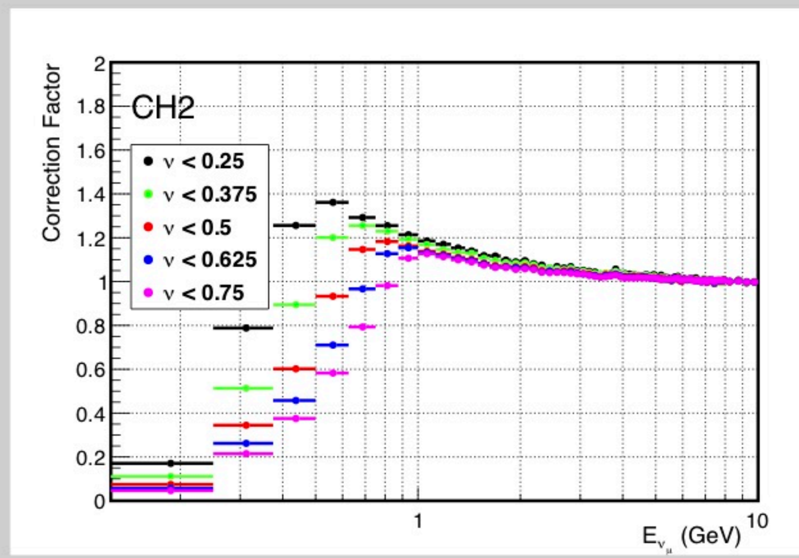

Detector response

We simulated an acceptance of 80% and a energy resolution of 5% to test the unfolding and the analysis procedure

Detector simulation and event reconstruction on going

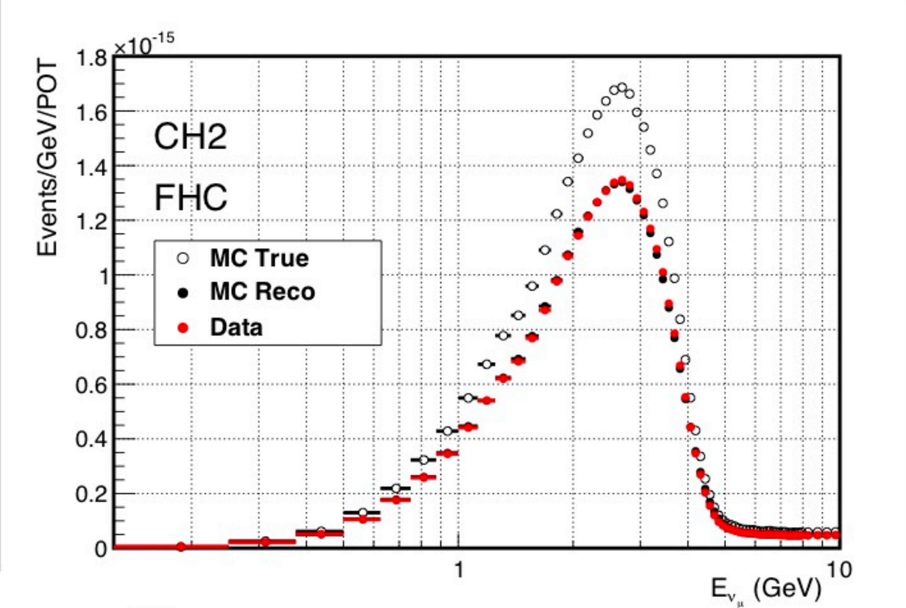

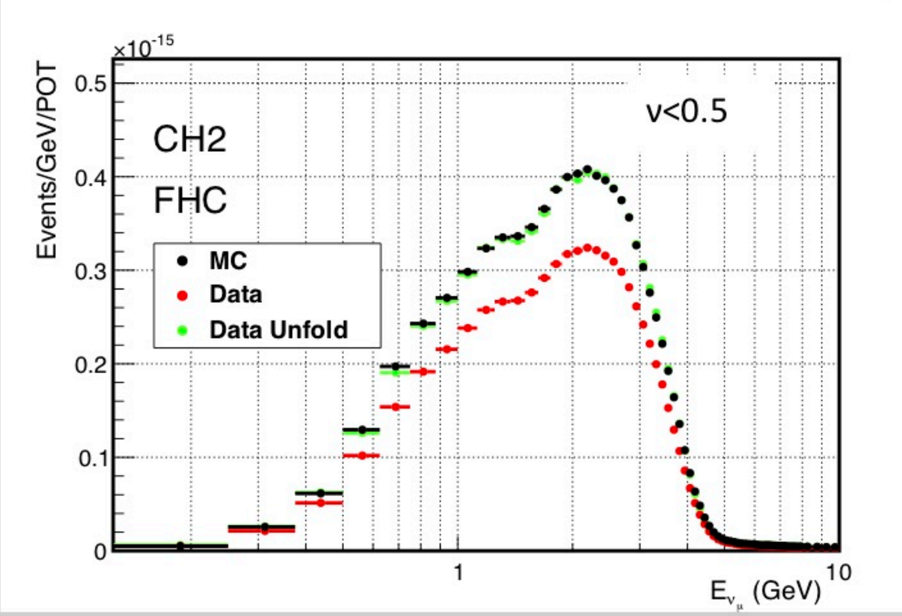

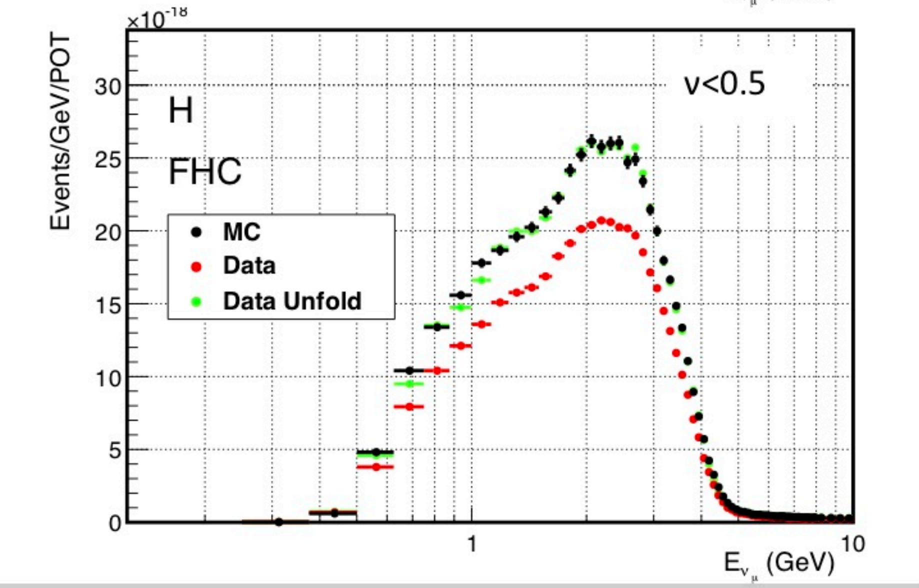

Relative fluxes

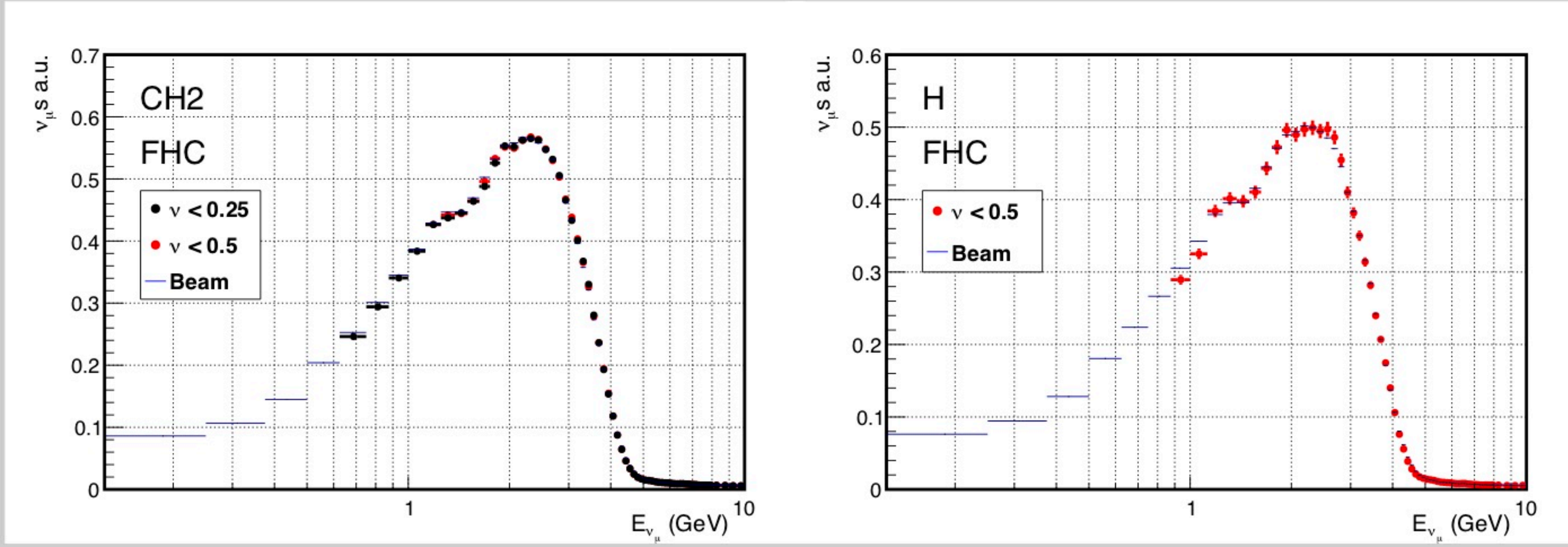

RHC mode: anti-neutrinos

CH$_2$			
ν_0 (GeV)	E_{min} (GeV)	$N^{\nu}_{int}/5.5 \cdot 10^{21}$ POT	N^{ν}_{int}/N_{int}
0.250	1.125	$2.28 \cdot 10^6$	0.22
0.375	1.500	$2.75 \cdot 10^6$	0.26
0.500	2.125	$2.69 \cdot 10^6$	0.25
0.625	2.750	$2.03 \cdot 10^6$	0.19
0.750	3.375	$1.19 \cdot 10^6$	0.11
H			
ν_0 (GeV)	E_{min} (GeV)	$N^{\nu}_{int}/5.5 \cdot 10^{21}$ POT	N^{ν}_{int}/N_{int}
0.250	1.750	$5.29 \cdot 10^5$	0.27
0.375	2.250	$4.86 \cdot 10^5$	0.25
0.500	2.875	$3.35 \cdot 10^5$	0.17
0.625	3.375	$2.12 \cdot 10^5$	0.11
0.750	3.875	$1.20 \cdot 10^5$	0.06

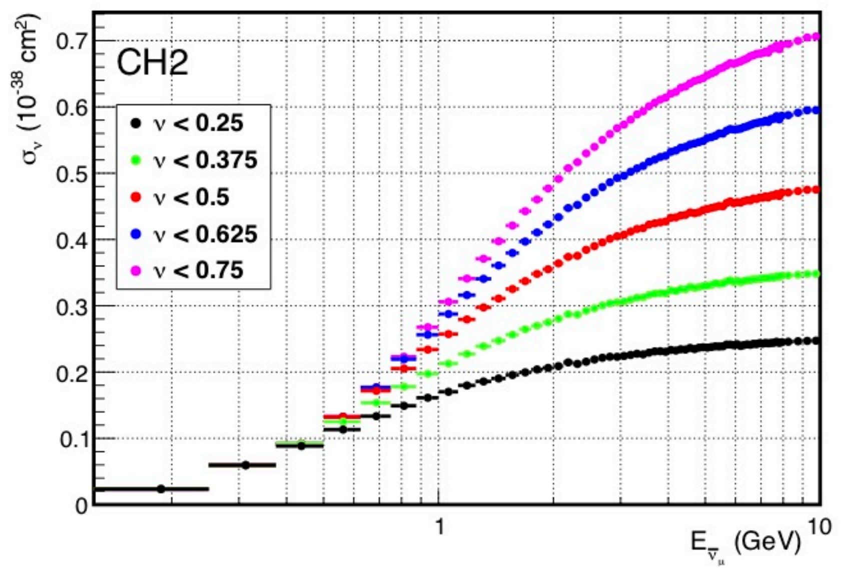

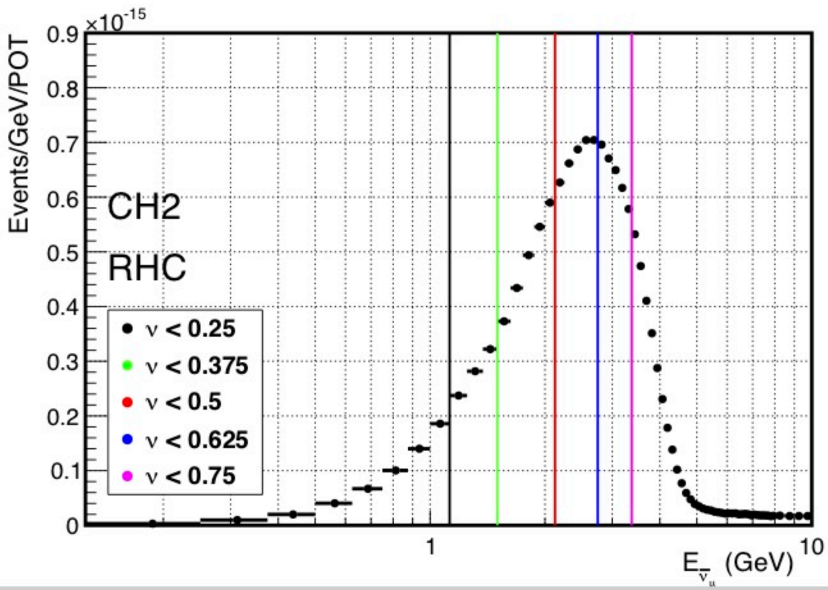

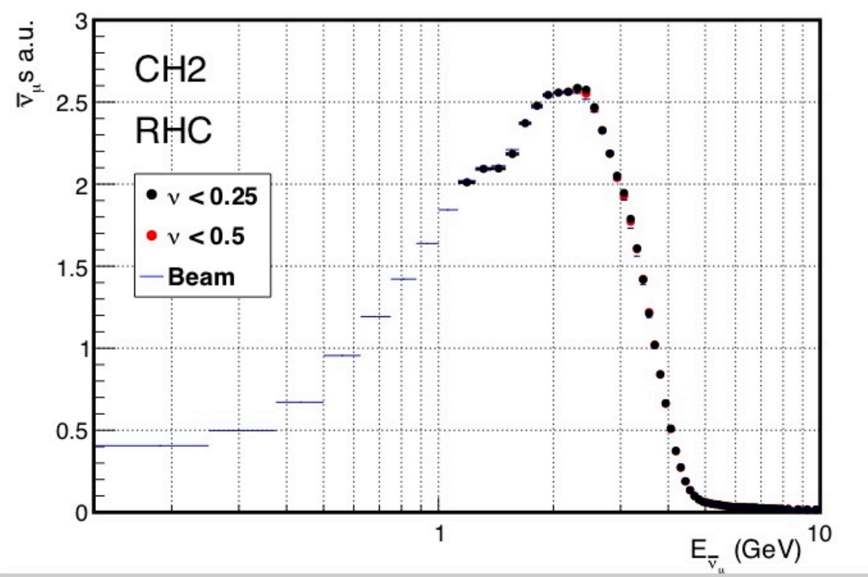

Next steps…

- Simulate the detector response:
    - particle and event reconstruction
    - particle identification
    - background
- Improve the the unfolding procedure
- Optimize the analysis (low-nu cut values, energy thresholds…)

PRISM-like exposure

Beam profile simulation:
We implemented the simulation of neutrino events according to beam fluxes determined through a 2D energy-position matrix and choosing an off-axis alignment for the detector.

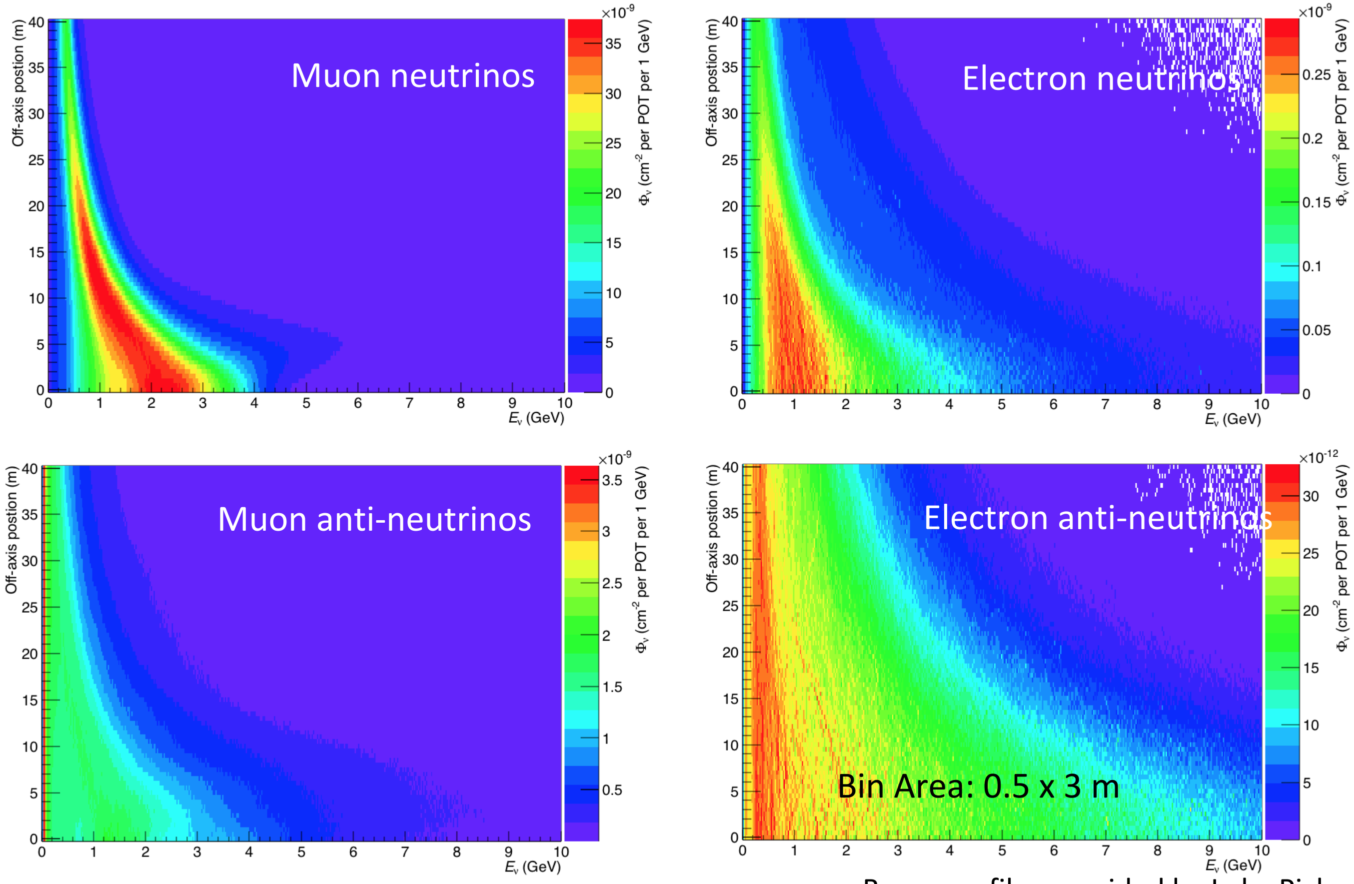

Beam profiles provided by Luke Pickering

Interaction rate

Internal LAr target (1.01 ton mass)

Seven different positions, including the on-axis alignment, were simulated.

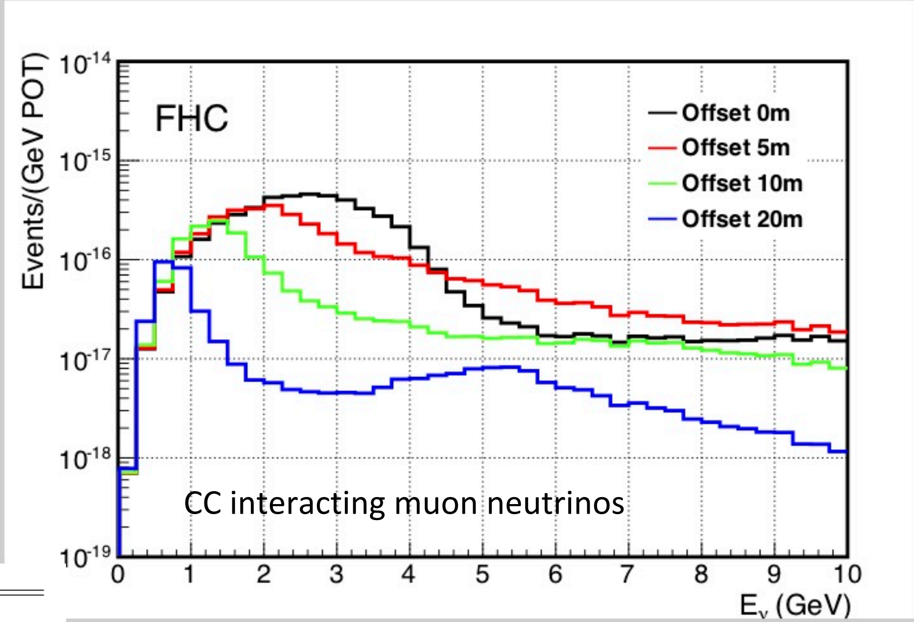

Equal POTs at each position						
Offset	10^{20} POT	CCInc ν_μ	NCInc	CCInc $\bar{\nu}_\mu$	CCInc ν_e	El. ν_μ-e
0 m	0.786	$9.4 \cdot 10^4$	$3.4 \cdot 10^4$	$2.9 \cdot 10^3$	$1.1 \cdot 10^3$	8.5
5 m	0.786	$7.3 \cdot 10^4$	$2.6 \cdot 10^4$	$2.5 \cdot 10^3$	$9.3 \cdot 10^2$	6.3
10 m	0.786	$3.2 \cdot 10^4$	$1.2 \cdot 10^4$	$1.5 \cdot 10^3$	$6.1 \cdot 10^2$	2.7
15 m	0.786	$1.4 \cdot 10^4$	$5.5 \cdot 10^3$	$8.0 \cdot 10^2$	$3.9 \cdot 10^2$	1.3
20 m	0.786	$7.9 \cdot 10^3$	$3.2 \cdot 10^3$	$5.2 \cdot 10^2$	$2.5 \cdot 10^2$	0.7
25 m	0.786	$4.8 \cdot 10^3$	$2.0 \cdot 10^3$	$3.4 \cdot 10^2$	$1.7 \cdot 10^2$	0.4
30 m	0.786	$3.1 \cdot 10^3$	$1.3 \cdot 10^3$	$2.5 \cdot 10^2$	$1.2 \cdot 10^2$	0.3
All	5.500	$2.3 \cdot 10^5$	$8.4 \cdot 10^4$	$8.8 \cdot 10^3$	$3.6 \cdot 10^3$	20.2
Half POTs on-axis						
Offset	10^{20} POT	CCInc ν_μ	NCInc	CCInc $\bar{\nu}_\mu$	CCInc ν_e	El. ν_μ-e
0 m	2.750	$3.3 \cdot 10^5$	$1.2 \cdot 10^5$	$1.0 \cdot 10^4$	$4.0 \cdot 10^3$	29.6
5 m	0.458	$4.2 \cdot 10^4$	$1.5 \cdot 10^4$	$1.5 \cdot 10^3$	$5.4 \cdot 10^2$	3.7
10 m	0.458	$1.9 \cdot 10^4$	$6.8 \cdot 10^3$	$9.0 \cdot 10^2$	$3.6 \cdot 10^2$	1.6
15 m	0.458	$8.5 \cdot 10^3$	$3.2 \cdot 10^3$	$4.7 \cdot 10^2$	$2.3 \cdot 10^2$	0.7
20 m	0.458	$4.6 \cdot 10^3$	$1.9 \cdot 10^3$	$3.0 \cdot 10^2$	$1.5 \cdot 10^2$	0.4
25 m	0.458	$2.8 \cdot 10^3$	$1.2 \cdot 10^3$	$2.0 \cdot 10^2$	$9.7 \cdot 10^1$	0.3
30 m	0.458	$1.8 \cdot 10^3$	$7.7 \cdot 10^2$	$1.4 \cdot 10^2$	$6.8 \cdot 10^1$	0.2
All	5.500	$4.1 \cdot 10^5$	$1.5 \cdot 10^5$	$1.3 \cdot 10^4$	$5.4 \cdot 10^3$	36.5

Two different run plans:
equal POTs dedicated at each position, including the on-axis alignment and half POTs on-axis.

Detector response and analysis on going.